Journal of Magnetism and Magnetic Materials 491 (2019) 165604

Contents lists available at ScienceDirect

Journal of Magnetism and Magnetic Materials

journal homepage: www.elsevier.com/locate/jmmm

Research articles

Effect of external magnetic field on cyclic voltammetry of exfoliated graphene-based magnetic composites with conductive polymer and carbon dots

Mahmoud M.M. Ahmed[a], Toyoko Imae[a,b,*]

[a] Graduate Institute of Applied Science and Technology, National Taiwan University of Science and Technology, Keelung Road, Taipei 10607, Taiwan, ROC
[b] Department of Chemical Engineering, National Taiwan University of Science and Technology, Keelung Road, Taipei 10607, Taiwan, ROC

ARTICLE INFO

Keywords:
Magnetic graphene composite
Iron oxide nanoparticle
Polyaniline
Carbon dot
External magnetic field
Cyclic voltammetry
Supercapacitor

ABSTRACT

Cyclic voltammetric performance of magnetic graphene composites expanded at 90, 900 and 2000 °C and their composites with polyaniline and carbon dots was monitored under external magnetic fields at maximum 1191 Gauss generated from 7 A current supply. These composites showed the enhanced performances accompanied by the increase of magnetic field strength. The enhancement of the capacitance was further achieved, when iron oxide nanoparticles were further added on magnetic graphene composites, when polyaniline was in-situ combined with magnetic graphene composites or when carbon dot was hydrothermally loaded on magnetic graphene composites. These results clarify the remarkable effect of the external magnetic field on the electrochemical performance of magnetic graphene composites. This research should offer a breakthrough on the adoption of the magnetic field in energy science and technology.

1. Introduction

Nowadays magnetic nanoparticles play very important roles in many fields. Especially, the use of magnetic nanoparticles is remarkable in medical fields including drug delivery systems [1], magnetic resonance imaging [2–4], hyperthermia [5], computed tomography, tissue engineering and other techniques [6]. The use of the magnetic properties in these medical techniques enables an accurate sensing, diagnosis and treatment of many diseases [7]. Moreover, in the industrial applications, chemical sensor [8], catalysis [9], data storage [10], recycling and water purification [11] are among chief applications of the magnetic nanoparticles. Besides, the magnetic materials have successfully contributed to existential applications including telephone systems [12], magnetic cards and maglev vehicles. Nevertheless, they are still out-of-focus elements for the energy-related applications except a few cases [13] and thus their common usage on energy systems is challengeable due to their less conductivity compared to rare earth metals [14]. However, when the magnetic materials are hybridized with graphene-based carbon materials, the composite can exert high performance for supercapacitor [15].

We have exfoliated the $FeCl_3$-graphite intercalation compounds (GIC) by means of alkyl amine, followed by rapid heating at 900 °C in air and then 2000 °C in argon atmosphere [16–18]. The obtained non-defective graphene sheets displayed the capacitance properties contributed by the degree of exfoliation. Meanwhile, the as-prepared graphene sheets possessed superparamagnetic properties due to the remaining iron oxide nanoparticles and thus this character might be useful to raise electrochemical properties under the magnetic flux. Up to now, there is only one report where an external 720 Gauss of magnetic field was applied on graphene and magnetic graphene composites [19].

Herein, cyclic voltammetric (CV) investigations were performed for thermally exfoliated magnetic graphene composites with the superparamagnetic properties derived by coexisting iron oxide nanoparticles under the addition of suitable external magnetic fields. Then, the electrochemical performance of magnetic graphene composite is expected upon applying external magnetic field. Moreover, magnetic graphene composites were hybridized with conductive polymer (polyaniline, PANI), carbon dots and Fe_3O_4 nanoparticles and investigated under the external magnetic fields. These investigations will provide a very simple, easy and effective way for enhancing the capacitance performance of the magnetic graphene composites.

* Corresponding author at: Graduate Institute of Applied Science and Technology, National Taiwan University of Science and Technology, Keelung Road, Taipei 10607, Taiwan, ROC.
E-mail address: imae@mail.ntust.edu.tw (T. Imae).

https://doi.org/10.1016/j.jmmm.2019.165604
Received 21 January 2019; Received in revised form 8 July 2019; Accepted 17 July 2019
Available online 17 July 2019

2. Experimental section

2.1. Reagents and instruments

Indium tin oxide (ITO) glass was purchased from Uni-Onward Co. Polyvinylidene fluoride was a product from Sigma Aldrich. N-methylpyrrolidone, aniline, ammonium persulfate, citric acid and ethylenediamine were purchased from Acros organics. $FeCl_3{\cdot}6H_2O$, $FeCl_2{\cdot}4H_2O$, and an ammonia solution were purchased from Sigma Aldrich, Alfa Aesar and Fisher scientific, respectively. All materials were used as provided.

Morphological images were captured by field emission scanning electron microscopy (FE-SEM) (JEOL JSM6500F) at an accelerating voltage of 10 kV. The spacemen were sputtered by platinum nanoparticles before the measurement to allow better resolutions. The nitrogen adsorption-desorption isotherms were examined using BELSORB MAXI, Japan. The samples were degassed at 300 °C for 3 h under vacuum condition prior to measurement.

2.2. Preparation of composites

Exfoliated magnetic graphene compounds are same as previously synthesized and characterized ones: The product by amine-exfoliation of stage-1 $FeCl_3$-GIC [16] was named G-90, the heat-exfoliated product at 900 °C from G-90 [17] was called G-900 and G-900 heated at 2000 °C under inert atmosphere was termed G-2000 [18]. G-90, G-900 and G-2000 included iron components of 20, 40, and 10 wt%, respectively.

Aniline was in-situ polymerized on G-900 as the previous report [17]. Briefly, aniline was dispersed in ethanolic 1.0 M H_2SO_4 solution, G-900 and ammonium persulfate were then added to the dispersion and stirred for one day. The product named as G-900-PANI was filtered, rinsed by ethanol and dried overnight in vacuum at 50 °C.

G-900 (8 mg) was mixed with citric acid (800 mg) and ethylenediamine (400 µl) in water (50 ml). The mixtures were respectively heated at 183 °C for 16 h in an autoclave [20–22]. The product was filtered, washed, and dried in oven at 60 °C for 1 h. The products were named G-900-Cdot. The characterization of carbon dot was performed in the previous works [20–22].

G-90 (45 mg) were mixed with iron(III) chloride hexahydrate (140 mg) and iron(II) chloride tetrahydrate (70 mg), stirred in ethanol at room temperature for 2 h, followed by rapid addition of an ammonia solution to the mixture. The color of the reacting dispersion turned black once ammonia was added. The dispersion was continuously stirred for one day. The product was named G-90-Fe.

As-synthesized graphene-based materials and the synthesis routes are drawn in Scheme 1.

2.3. CV measurements under magnetic field

CV measurement was performed on a Zahner Zennium E electrochemical workstation. The working electrodes were prepared by mixing as-synthesized graphene-based composites (20 mg) with polyvinylidene fluoride (2.0 mg) in suitable amount of N-methylpyrrolidone. The mixture (slurry) was stirred, homogenized and dried on the ITO substrate [17,18].

The CV curves were measured in an aqueous electrolyte (1.0 M NaCl) solution at room temperature using a three-electrodes system with Ag/AgCl as a reference electrode and a platinum foil as a counter electrode. The cycling range was between −1.0 and 1.0 V, and the scan rates were varied from 5 mVs^{-1} to 30 Vs^{-1}.

The capacitance (C) was calculated according to the equation of C = i/s, where i is the average current density in Ag^{-1} unit and s is the sweep rate in s unit. The current density was calculated as the integration of area of CV curve. The values of current density and capacitance were normalized by the mass of the graphene-based composites, which were 1.0 ~ 1.5 mg on the 1.0 × 0.5 cm^2 ITO electrode.

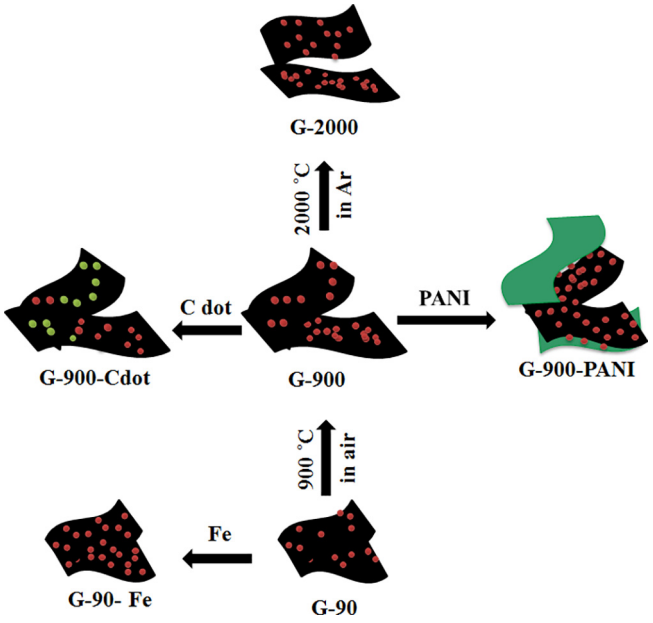

Scheme 1. A roadmap of synthesis of graphene-based composite materials.

The magnetic field was generated via small DC batteries that provide a stable and fine DC current. The battery was connected to a solenoid coil with a known fixed cycle number and length (65 cycle and 480 cm length). Different current batteries were equipped on the same coil. The coil was directly placed on the top of the electrochemical cell (Scheme 2). The magnetic field was applied simultaneously with CV measurement. The magnetic field was generated from different DC current supplies at 3, 5, 6, 6.5, 7 A, corresponding to 510, 850, 1020, 1106, 1191 Gauss, respectively. The calculation of the magnetic flux density H was based on an equation H = µ(IN)/L, where µ is the magnetic permeability constant, I is the applied current, N is the number of cycles of the solenoid and L is the length of the wire in the circuit. In this equation, if the coil is fixed, the magnetic field strength is mainly dependent on the applied current and, therefore, the applied current can be described instead of the magnetic field strength. The measurement was performed at room temperature and atmospheric pressure.

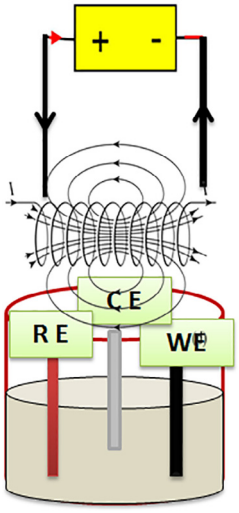

Scheme 2. An electrochemical cell equipped with magnetic field.

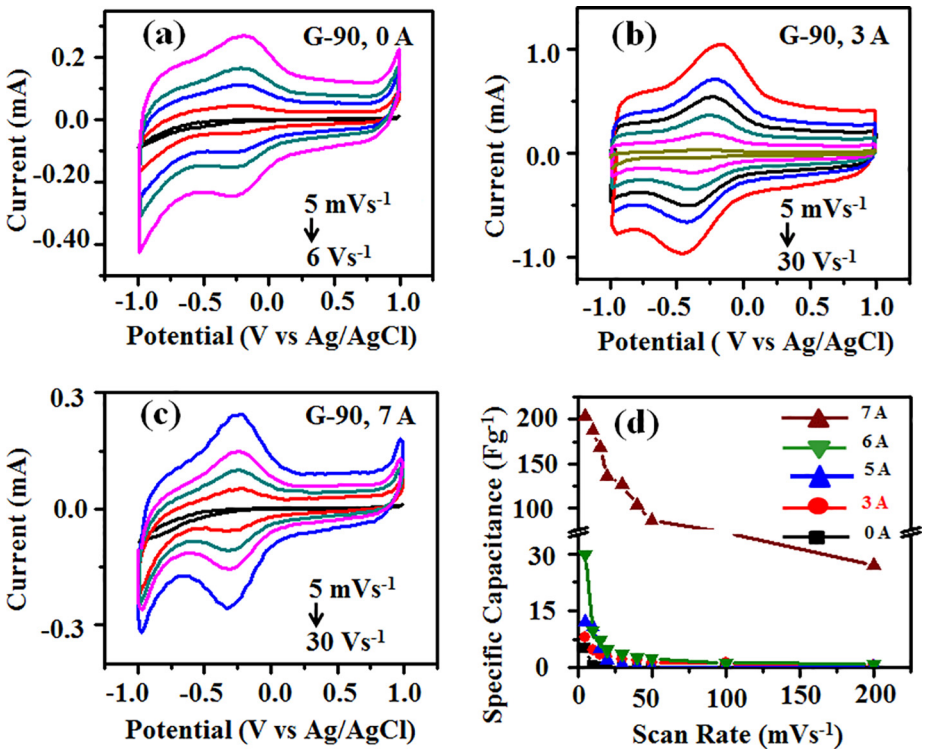

Fig. 1. CV curves for G-90 under (a) 0 A, (b) 3 A, and (c) 7 A current supplies. Scan rates were 5 mVs^{-1} to 6 Vs^{-1} for (a) and 5 mVs^{-1} to 30 Vs^{-1} for (b) and (c). (d) Specific capacitances at different current supplies as a function of scan rate.

3. Results and discussion

3.1. Effect of external magnetic field on cyclic voltammetry of exfoliated magnetic graphene composites

CV curves of G-90 were measured under magnetic fields from 0, 3, 5, 6 and 7 A current supplies. CV curves of G-90 without magnetic field showed both electric double layer capacitance (EDLC) and pseudocapacitor (PC) profiles in the range of $-1.0 \sim 1.0$ V with a minor PC performance at $-0.5 \sim 0$ V in all investigated scan rates (5 $mVs^{-1} \sim 6$ Vs^{-1}) (Fig. 1a). This PC performance became dominant with increasing the applied magnetic fields up to 7 A current supply as illustrated in Fig. 1b, c. Hence specific capacitance values were increased by increasing the applied current as seen in Fig. 1d, where the specific capacitances calculated from CV curves at different current supplies are plotted as a function of scan rate.

It should be noted that the specific capacitance at 7 A was remarkably higher than those at lower current supplies (Fig. 1d). In details, the specific capacitance at 5 mVs^{-1} was only 5 Fg^{-1} before applying magnetic field, but it reached 8, 12 and 30 Fg^{-1} in response to applied magnetic fields at 3, 5 and 6 A current supplies, respectively. Furthermore, it drastically increased to achieve 204 Fg^{-1} upon applying 7 A. That is, the applied magnetic fields increased the CV performance, being directly proportional to increase the specific capacitance.

Further examination of CV behaviors under magnetic field was performed for heat-exfoliated magnetic graphene composite (G-2000) (Fig. 2a, b). The applied magnetic field (3, 5 and 6 A) was effective on increasing the CV performance and generating the EDLC character superior to the PC property, being different from a case of G-90. At the same time, the applied magnetic field efficiently increased the achieved CV area at all investigated scan rates (5 $mVs^{-1} \sim 30$ Vs^{-1}) at different applied magnetic fields. These enhanced performances can be shown through the more quadrangular CV shapes at higher magnetic field and higher scan rate with a stable electrode efficiency. Against the specific capacitance (90 Fg^{-1} at 5 mVs^{-1}) of G-2000 without applying any external magnetic field [18], the capacitance at the same scan rate achieved 130, 153 and 469 Fg^{-1}, upon applying 3, 5 and 6 A, respectively (Fig. 2c). These results indicated 144, 170 and 521% increase, respectively, compared to the result for G-2000 without applying magnetic field.

The electrochemical performance under the effect of the magnetic field has been reported by Zhu et al. [19], who have applied the magnetic field through a sophisticated instrument to allow a stable current flow and obtained the capacitance values of 50 Fg^{-1} at scan rate of 2 mVs^{-1} for the electrode consisting of iron oxide nanoparticles anchored on the functional groups of graphene oxide. The magnetic nanoparticles allow the effect of the external magnetic field on the electrochemical cell. Herein, the external magnetic field was applied through a homemade electric circuit connected to a known solenoid coil, which provided a cheap and effective magnetic field supply. Moreover, the graphene (G-90, G-900 or G-2000) used in the present investigation does not have any defects or functional groups, and the iron oxide nanoparticles existed within the graphene layers. This stable coexistence allows the composite to be more durable and efficient for energy storage and provides better performance and stability under a severe magnetic field condition.

3.2. Effect of external magnetic field on cyclic voltammetry of exfoliated magnetic graphene composites with additives

Exfoliated magnetic graphene composites were hybridized with additives such as Fe_3O_4 nanoparticles, conductive polymers and carbon dots, and the CV performance of the hybrids under the external magnetic field were compared, since the synergetic effect of polyaniline on carbon material and the enhancement of iron-based nanoparticles and carbon dots on supercapacitor have been reported [20,21].

G-90 was hybridized by depositing additively iron oxide nanoparticles. Under different magnetic fields, the CV curves of an obtained composite (G-90-Fe) showed at least two-pair redox peaks dominated

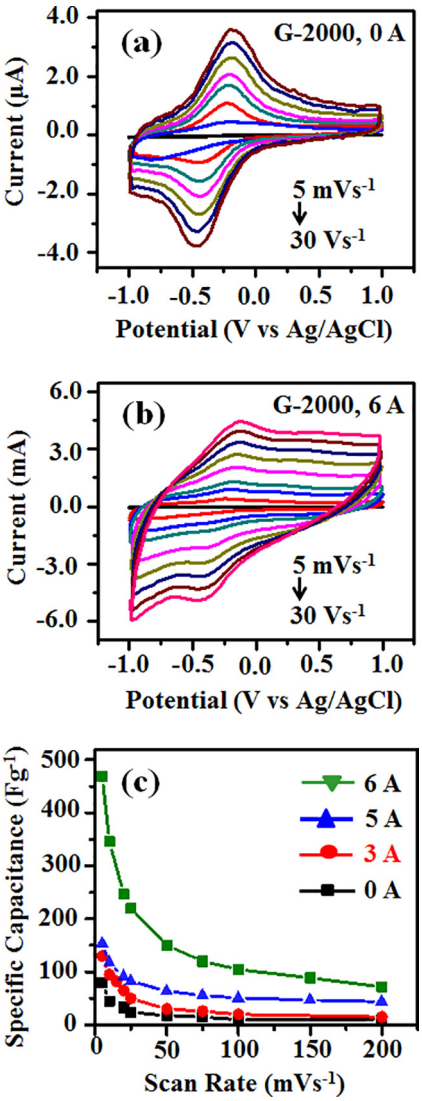

Fig. 2. CV curves for G-2000 at scan rates of 5 mVs^{-1} to 30 Vs^{-1} under (a) 0 A and (b) 6 A current supplies. (c) Specific capacitance at different current supplies as a function of scan rate.

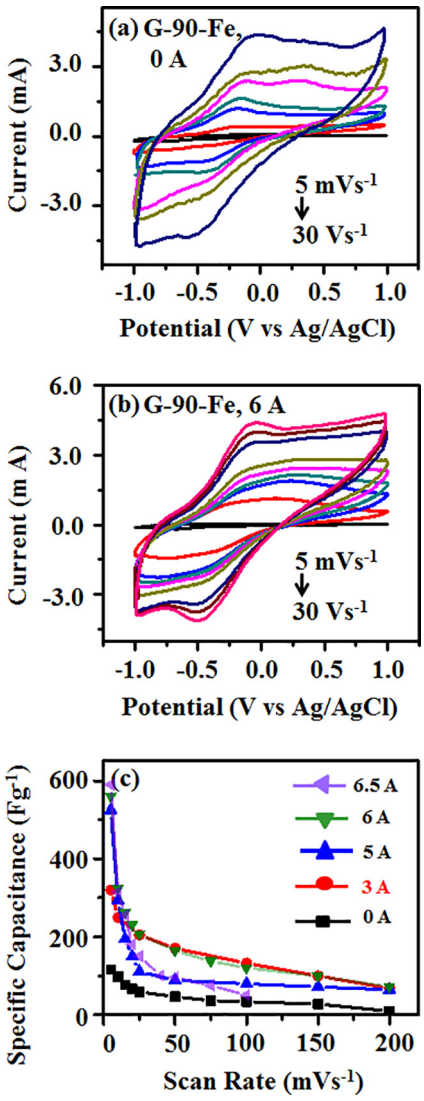

Fig. 3. CV curves for G-90-Fe at scan rates of 5 mVs^{-1} to 30 Vs^{-1} under (a) 0 A and (b) 6 A current supplies. (c) Specific capacitance at different current supplies as a function of scan rate.

by the PC behavior (Fig. 3a, b). During the charge/discharge cycles, redox peaks at higher potential were diminished and redox peaks at lower potential became predominant. These two pairs may originate from two types of magnetite; One is incorporated on the process of the synthesis of graphene from $FeCl_3$-GIC and another is additionally incorporated to prepare G-90-Fe. While G-90-Fe without the addition of any magnetic field achieved the specific capacitance of 116 Fg^{-1} at 5 mVs^{-1}, the capacitance under the magnetic field reached 320, 525, 560, 590 Fg^{-1} at the same scan rate under 3, 5, 6 and 6.5 A current supplies, respectively (Fig. 3c). These results indicate the predominant effect of the magnetic field on the magnetite-rich composites in comparison of the pristine magnetic graphene composites. In other words, the higher content of magnetite drives the higher efficiency of the magnetic field.

The hybrid of G-900 with PANI achieved an efficient performance of specific capacitance of 253 Fg^{-1} at 5 mVs^{-1} [17], and this capacitance was 6 times higher than that (42 Fg^{-1} at 5 mVs^{-1}) of pristine G-900 [17]. Under the magnetic field from 7 A current supply, the CV curves of G-900-PANI were quite similar to those of G-900 and displayed rather EDLC feature at all investigated scan rates (5 $mVs^{-1} \sim 30$ Vs^{-1}), and the achieved capacitance value of the composite was almost double (525 Fg^{-1} at 5 mVs^{-1}) compared to it without magnetic field (Fig. 4). It is estimated that the magnetic nanoparticles embedded in the G-900 agitate the effect of the magnetic field to reach the capacitance performance in addition to the enlargement of capacitance by conductive PANI. Although the addition of PANI (PC material) to graphene-based compound (EDLC material) has been reported to enhance the capacitance [17,20], it was proved in the present work that the capacitance can be further enhanced under the magnetic field.

Because carbon dot is an allotrope of graphitic carbons and possesses the quantum character, carbon dot is effective for enhancing the biomedical, chemical and physical properties [20–22]: The addition of carbon dot decreased the band gap of semiconductive materials and intensified the capacitance of conductive polymers. Alternatively, G-900 was hybridized with carbon dot and investigated its CV curves (Fig. 5). The achieved CV curves of G-900-Cdot showed the efficient capacitance activity at all investigated scan rates (5 $mVs^{-1} \sim 5$ Vs^{-1}). The CV shapes were identical with the EDLC-major shape at 0 A current supply but added the PC feature with increasing the applied magnetic flux (Fig. 5a, b). Moreover, the capacitance values reached 67, 73, 165, 200 and 225 Fg^{-1} at 5 mVs^{-1} under 0, 3, 5, 6 and 7 A current supplies, respectively. These capacitance values indicated the effect of the external magnetic field on the electrochemical performances. The specific capacitance values at 5 mVs^{-1} for all composites examined in this work

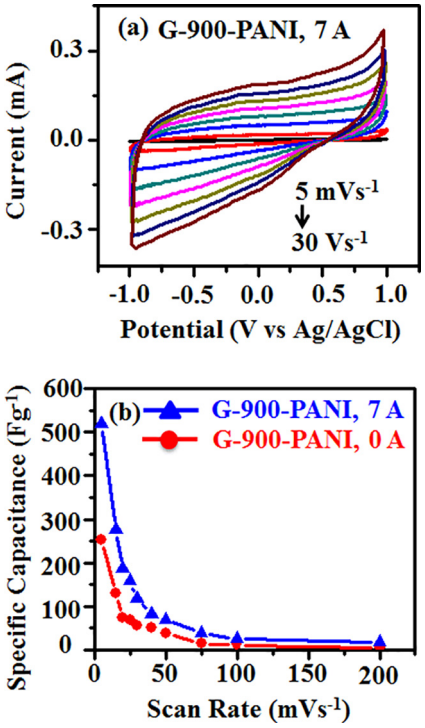

Fig. 4. (a) CV curves for G-900-PANI at scan rates of 5 mVs^{-1} to 30 Vs^{-1} under 7 A current supply. (b) Specific capacitance at a 7 A current supply as a function of scan rate.

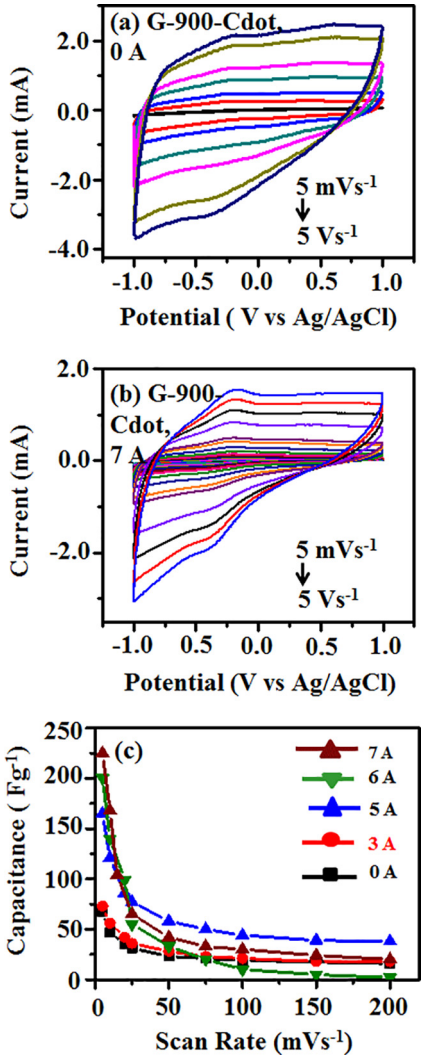

Fig. 5. (a) CV curves for G-900-Cdot at scan rates of 5 mVs^{-1} to 5 Vs^{-1} under (a) 0 A and (b) 7 A current supplies. (b) Specific capacitance at different current supplies as a function of scan rate.

are listed in Table 1 and displayed graphically in Fig. 6.

In addition, the columbic (faradaic) efficiency of G-90, G-2000 and G-900-Cdot under the magnetic field was investigated at 20 Ag^{-1} for 9000 cycles (Fig. 7). The stability of G-90 under 7 A reached 99%, and G-2000 achieved 96% under 6 A. Moreover, even G-900-Cdot at 6 A achieved the capacitive retention of 95%. All these results confirm the stable contribution of the magnetic field on the electrochemical performance of magnetic graphene composites.

The charge transfer rate studies were tested through the electrochemical impedance spectroscopy (EIS). The EIS curves (Fig. 8) of the magnetic materials on ITO glass were investigated within the frequency range 100 mHz to 100 kHz at the open circuit potential and 5 mV as an amplitude. It should be noticed that the semi circuit region indicates the electron transfer resistance of the material [20,21]. This phenomenon was clearly observed in G-900, G-900-PANI and G-900-Cdots, whereas G-90 and G-90-Fe didn't show such behavior and the behavior of G-2000 was between two cases. The simulation circuit composed of four elements of the series resistance (R_s), the charge-transfer resistance (R_{ct}), the electrical double-layer capacitance (C_{dl}), and Warburg diffusion impedance (W_d), as displayed in the inset of Fig. 8. The values of series resistance and charge transfer resistance are listed in Table 1. The values of the electron transfer resistance were higher in the order of G-90, G-900 and G-2000 and the additives increased the electron transfer resistance. These results indicate that the charge transfer rate of the present magnetic materials is inverse of their electrochemical performances. Thus, the motivation for enhancing specific capacitance should be another factor except the charge transfer. The variation of series resistance was also independent of the variation of the electrochemical performance, although the additives on G-90 or G-900 decreased the series resistance, indicating the faster charge transfer and thus the affecting on the capacitance increase.

The morphologies of magnetic compounds were examined through FE-SEM (see Fig. 9). While G-90 is a plat sheet [16] and Fe_3O_4 is a spherical particle of around 9 nm size, the images of G-90-Fe showed a granular structure of 300–500 nm. Granules may be formed from Fe_3O_4 particles wrapped with G-90 sheet. However, G-900-PANI maintained the obvious sheet structure alike G-900, although the pristine PANI took an amorphous structure [20]. PANI should have preferably stuck to a

Table 1
Lists of specific capacitances under the different applied current supplies, capacitance retention, resistance and specific surface area of composites.

Material	G-90	G-90-Fe	G-900	G-900-PANI	G-900-Cdot	G-2000
Specific capacitance (Fg^{-1}) at 5 mVs^{-1}						
0 A	5	116	42	253	67	90
3 A	8	320	–	–	73	130
5 A	12	525	–	–	165	153
6 A	30	560	–	–	200	469
6.5 A	–	590	–	–		–
7 A	204	–		521	225	–
Capacitance retention (%)	99 (at 7 A)				95 (at 6 A)	96 (at 6 A)
series resistance (Ω)	76.9	26.2	48.5	120.5	35.8	36.6
Charge transfer resistance (Ω)	17.7	19.5	18.3	84.0	35.7	32.5
Specific surface area (m^2g^{-1})	0.5	4	17	24	40	53

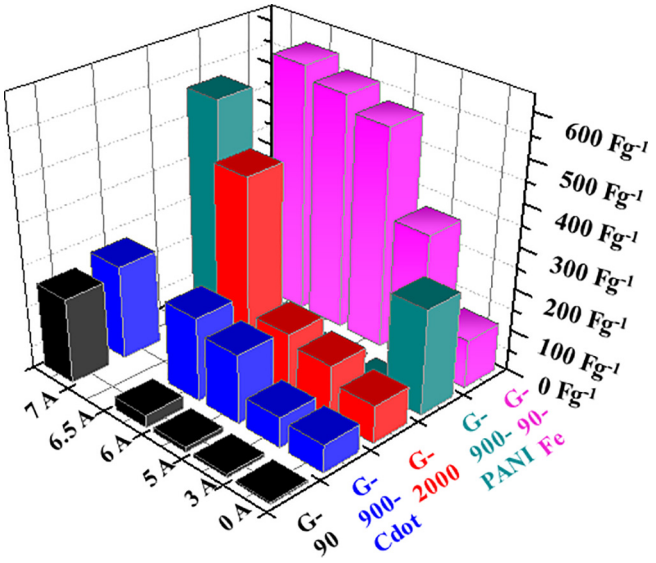

Fig. 6. Graphical display of specific capacitance of composites at 5 mVs^{-1} under the applied current supplies.

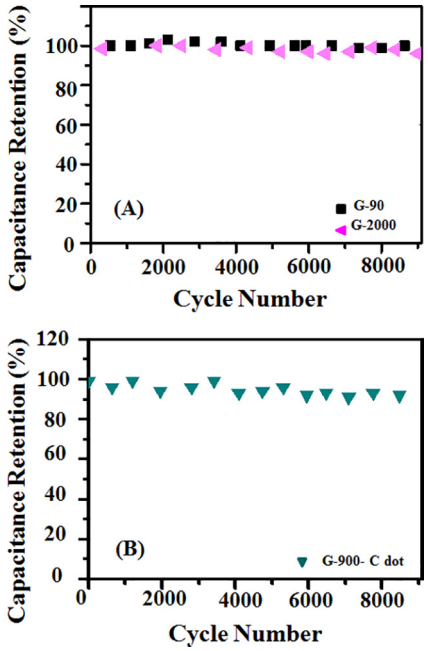

Fig. 7. Capacitance retention at 20 Ag^{-1} for G-90 at 7 A and G-2000 and G-900-Cdot at 6 A.

graphene sheet. Thus, this morphology variation after combined with Fe_3O_4 or PANI may be involved to the electrochemical performances and allow the enhanced capacitance under the applied magnetic fields.

The N_2 adsorption-desorption isotherms are plotted in Fig. 10. The isotherms of G-90-Fe, G-900-PANI and G-900-Cdot showed a non-porous structure of type II similar to G-90 and G-900 [17], and their surface areas reached 4, 24, and 40 m^2g^{-1}, respectively. Thus, the addition of Fe_3O_4, Cdot and PANI increased the specific surface area, confirming the contribution of specific surface area to the enhancement of specific capacitance.

4. Conclusions

An external magnetic field was applied on electrochemical cells of iron oxide-composited graphene composites. This technique was developed to achieve the best result using homemade DC current source connected to a specific solenoid coil of known parameters. Upon applying external magnetic field, the electrochemical performance of magnetic graphene composite was noted. It was found that all magnetic

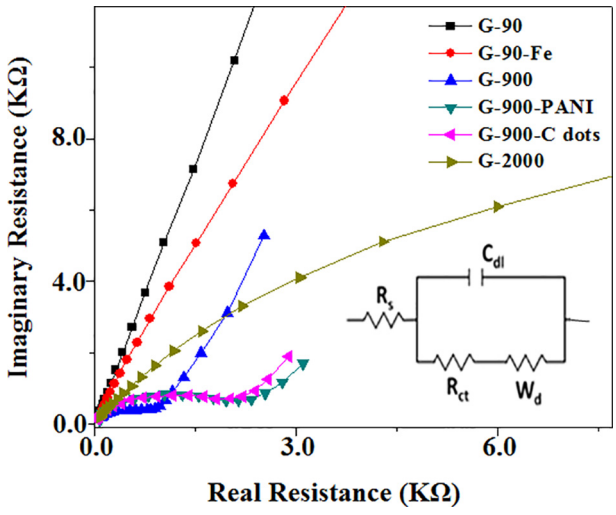

Fig. 8. Electrochemical impedance spectroscopy (EIS) of the magnetic compounds. Inset is the Randles Cell.

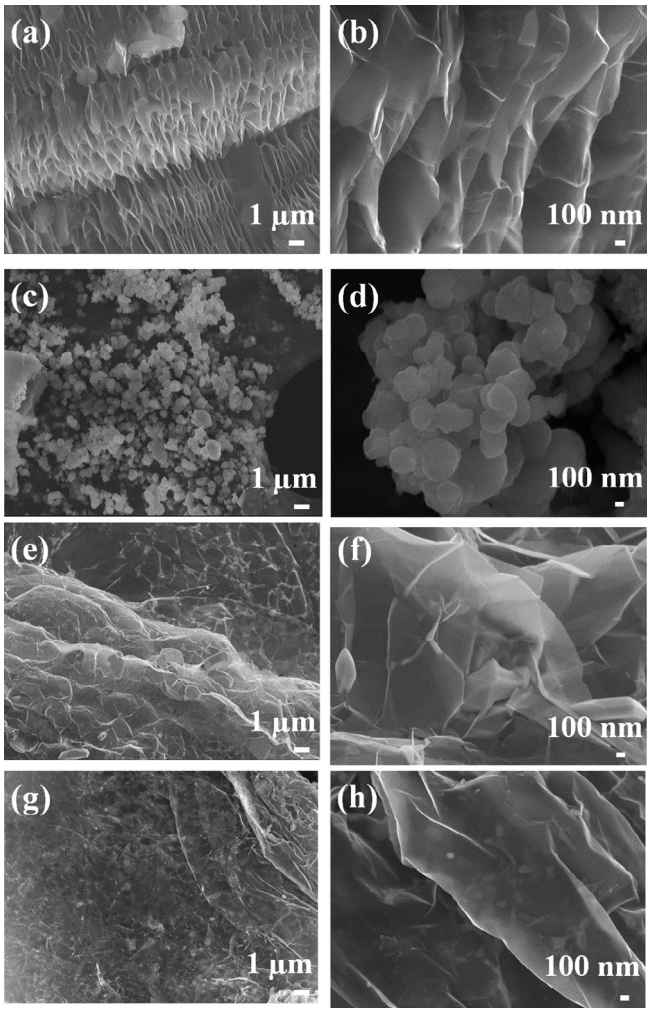

Fig. 9. FE-SEM images of (a, b) G-90, (c, d) G-Fe-90, (e, f) G-900 and (g, h) G-900-PANI.

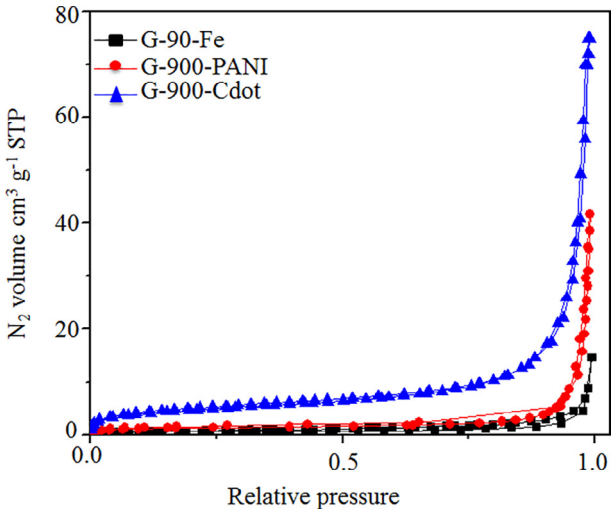

Fig. 10. N_2 adsorption-desorption isotherms of G-90-Fe, G-900-PANI and G-900-Cdot.

graphene composites showed a distinct enhancement under the effect of the magnetic field. The development under 7 A current supply reached 40 times higher capacitance value at 5 mVs^{-1} for G-90 than the pristine value without magnetic field due to the existence of the magnetic nanoparticles. Similarly, the achieved capacitance was drastically increased to reach 521% for G-2000 at 5 mVs^{-1} under 6 A against without magnetic field. Moreover, when G-900 were hybridized with carbon dot and the 6 A energy supply was applied, the achieved capacitance reached 200 Fg^{-1} at 5 mVs^{-1}. These results visibly showed the strong effect of the magnetic field to enhance the electrochemical performance of magnetic graphene composites.

It is well-established that the magnetic field could enhance the energy state of the electrons [23]. Hence, the electron transportation capability will be enhanced and the EDLC resulting from graphene will be improved [24]. In other words, the external application of magnetic field allows the enhancement of the EDLC performance. This enhancement is expected to be caused by the higher exfoliation of graphene layers, leading to the expanded area for electron transportation and enhancing the PC effect, since iron oxides are exposed to the larger electron-transporting area [25]. Thus, the applied high magnetic field plays a role of facile electron transport, which allows easy accessibility of the electrolyte ions to the electrode through graphene. These results introduce new methods for enhancing the electrochemical properties of magnetic composites under the effect of an external magnetic field in energy storage applications. In addition, this idea can provide a useful hint for new creative applications of magnetic field in various nanotechnologies.

Acknowledgements

This research was partially supported by Ministry of Science and Technology (MOST 106-2221-E-011-121-), Taiwan. MMMA gratefully acknowledges the financial support by a student scholarship and a postdoctoral fellowship from National Taiwan University of Science and Technology, Taiwan.

References:

[1] M.B. Zakaria, A.A. Belik, C.-H. Liu, H.-Y. Hsieh, Y.-T. Liao, V. Malgras, Y. Yamauchi, K. Wu, Prussian blue derived nanoporous iron oxides as anticancer drug carriers for magnetic-guided chemotherapy, Chem. Asian J. 10 (2015) 1457–1462.
[2] B. Thiesen, A. Jordan, Clinical applications of magnetic nanoparticles for hyperthermia, Int. J. Hyperthermia 24 (2008) 467–474.
[3] T.-H. Shin, Y. Choi, S. Kim, J. Cheon, Recent advances in magnetic nanoparticle-based multi-modal imaging, Chem. Soc. Rev. 44 (2015) 4501–4516.
[4] Y.-H. Hsu, H.-L. Hsieh, G. Viswanathan, S.H. Voon, et al., Multifunctional carbon-coated magnetic sensing graphene oxide-cyclodextrin nanohybrid for potential cancer theragnosis, J. Nanoparticle Res. 19 (2017) 359.
[5] A. Ito, M. Shinkai, H. Honda, T. Kobayashi, Medical application of functionalized magnetic nanoparticles, J. Biosci. Bioeng. 100 (2005) 1–11.
[6] K.K. Cheng, P.S. Chan, S. Fan, S.M. Kwan, K.L. Yeung, Y.-X.J. Wáng, A.H.L. Chow, E.X. Wu, L. Baum, Curcumin-conjugated magnetic nanoparticles for detecting amyloid plaques in Alzheimer's disease mice using magnetic resonance imaging (MRI), Biomaterials 44 (2015) 155–172.
[7] T. Knopp, M. Erbe, S. Biederer, T.M. Sattel, T.M. Buzug, Efficient generation of a magnetic field-free line, Med. Phys. 37 (2010) 3538–3540.
[8] G. Li, V. Joshi, R.L. White, S.X. Wang, J.T. Kemp, C. Webb, R.W. Davis, S. Sun, Detection of single micron-sized magnetic bead and magnetic nanoparticles using spin valve sensors for biological applications, J. Appl. Phys. 93 (2003) 7557–7559.
[9] R. Dalpozzo, Magnetic nanoparticle supports for asymmetric catalysts, Green Chem. 17 (2015) 3671–3686.
[10] L. Wu, P.-O. Jubert, D. Berman, W. Imaino, A. Nelson, H. Zhu, S. Zhang, S. Sun, Monolayer assembly of ferrimagnetic $Co_xFe_{3-x}O_4$ nanocubes for magnetic recording, Nano Lett. 14 (2014) 3395–3399.
[11] R.D. Ambashta, M. Sillanpää, Water purification using magnetic assistance: a review, J. Hazard. Mater. 180 (2010) 38–49.
[12] V.E. Legg, Survey of magnetic materials and applications in the telephone system, Bell Sys. Tech. J. 18 (1939) 438–464.
[13] B. Balasubramanian, B. Das, R. Skomski, W.Y. Zhang, D.J. Sellmyer, Novel nanostructured rare-earth-free magnetic materials with high energy products, Adv. Mater. 25 (2013) 6090–6093.
[14] W. Wang, S. Guo, I. Lee, et al., Hydrous ruthenium oxide nanoparticles anchored to graphene and carbon nanotube hybrid foam for supercapacitors, Sci. Rep. 4 (4) (2014) 4452.
[15] Y. Gao, D. Wu, T. Wang, D. Jia, W. Xia, Y. Lv, Y. Cao, Y. Tan, P. Liu, One-step solvothermal synthesis of quasi-hexagonal Fe_2O_3 nanoplates/graphene composite as high performance electrode material for supercapacitor, Electrochim. Acta 191 (2016) 275–283.
[16] M. Ujihara, M.M.M. Ahmed, T. Imae, Y. Yamauchi, Massive-exfoliation of magnetic graphene from acceptor-type GIC by long-chain alkyl amine, J. Mater. Chem. A 2 (2014) 4244–4250.
[17] M.M.M. Ahmed, T. Imae, Electrochemical properties of a thermally expanded magnetic graphene composite with a conductive polymer, Phys. Chem. Chem. Phys. 18 (2016) 10400–10410.
[18] M.M.M. Ahmed, T. Imae, J.P. Hill, Y. Yamauchi, K. Ariga, L.K. Shrestha, Defect-free exfoliation of graphene at ultra-high temperature, Coll. Surf. A 538 (2018) 127–132.
[19] J. Zhu, M. Chen, H. Qu, Z. Luo, S. Wu, H.A. Colorado, S. Wei, Z. Guo, Magnetic field induced capacitance enhancement in graphene and magnetic graphene nanocomposites, Energy Environ. Sci. 6 (2013) 194–204.
[20] C.C. Chang, T. Imae, Synergistic performance of composite supercapacitors between carbon nanohorn and conducting Polymer, ACS Sustain. Chem. Eng. 6 (2018) 5162–5172.
[21] B. Devadas, T. Imae, Effect of carbon dots on conducting polymers for energy storage applications, ACS Sustain. Chem. Eng. 6 (2018) 127–134.
[22] Efa, T. Imae, Hybridization of carbon-dots with ZnO nanoparticles of different sizes, J. Taiwan Inst. Chem. Eng. 92 (2018) 112–117.
[23] I. Eremin, A.V. Chubukov, Magnetic degeneracy and hidden metallicity of the spin-density-wave state in ferropnictides, Phys. Rev. B 81 (2010) 024511.
[24] M.M. Ahmed, T. Imae, Nanolayer Research, Elsevier, Amsterdam, 2017, pp. 353–389 Chapter 10.
[25] E. Frackowiak, Carbon materials for supercapacitor application, Phys. Chem. Chem. Phys. 9 (2007) 1774–1785.